Science and Technology Indonesia
e-ISSN:2580-4391 *p*-ISSN:2580-4405
Vol. 9, No. 3, July 2024

Research Paper

Tapping into the Power of Sol-Gel Method for Enhanced Antimicrobial Activity of Titania Nanoparticles

Kormil Saputra[1,4], Masruroh Masruroh[1], Hendra Susanto[2*], Retna Apsari[3]

[1]*Department of Physics, Universitas Brawijaya, Malang, East Java, 65145, Indonesia*
[2]*Department of Biology, Universitas Negeri Malang, Malang, East Java, 65145, Indonesia*
[3]*Department of Physics, Universitas Airlangga, Mulyorejo, Surabaya, East Java, 60115, Indonesia*
[4]*Department of Physics, Universitas Mataram, Gomong, Mataram, West Nusa Tenggara, 83115, Indonesia*
***Corresponding author**: hendrabio@um.ac.id

Abstract
Increasing bacterial resistance to antibiotics has become a serious threat to global public health. In this context, this study aims to evaluate the antimicrobial activity of titanium dioxide nanoparticles (TiO_2 NPS) synthesized using the sol-gel method. TiO_2 NPS samples were prepared and characterized for morphology via field-emission scanning electron microscopy (FESEM) and X-ray diffraction (XRD) analysis. Kirby-Bauer disc diffusion method was used to test the antimicrobial activity of TiO_2 NPS against Gram positive bacteria *Staphylococcus aureus*, Gram negative bacteria *Escherichia coli*, and pathogenic fungus *Aspergillus penicillioides*. The results showed that TiO_2 NPS effectively inhibited the growth of microorganisms, with significant inhibition zones especially against fungi. The antimicrobial mechanism of TiO_2 NPS involves the formation of hydroxyl radicals and superoxide ions that damage the cell membrane of microorganisms. The implications of this study are the development of potential antimicrobial nanomaterials for biomedical and environmental applications, as well as the importance of considering the physical and chemical properties of TiO_2 NPS in designing effective infection treatment strategies.

Keywords
TiO_2 NPS, Antimicrobial Activity, Sol-Gel Method, Antimicrobial Resistance

Received: 30 January 2024, Accepted: 22 April 2024
https://doi.org/10.26554/sti.2024.9.3.546-555

1. INTRODUCTION

The emergence of infectious diseases poses a serious threat to global public health, especially with the rise of antibiotic-resistant bacterial strains (Fan et al., 2020; Sumardi et al., 2022). For many years, antibiotics have been the antidote to infections in community and hospital settings. Such infections are often associated with resistant organisms, such as Methicillin-Resistant *Staphylococcus aureus* (MRSA) (Halizah et al., 2023), penicillin-resistant *Streptococcus pneumoniae* (Albukhaty et al., 2022), multibiotic-resistant *Acinetobacter baumannii* (Alghamdi et al., 2022) and multibiotic-resistant *Pseudomonas aeruginosa* (Alhagri et al., 2023). Thus, new, more advanced antibacterial agents based on nanobiotechnology are needed. Thanks to their unique properties, nanoparticles (NPS) are often used in medical practice in the form of antimicrobial activity classified into various types, including carbon-based materials (such as fulerene and carbon nanotubes), inorganic nanoparticles (such as silver, palladium, and gold), metal oxides (such as aluminum oxide, titanium dioxide, zinc oxide, copper oxide and silicon oxide) and quantum dots (Ahmadpour Kermani et al., 2021; Alhagri et al., 2023; Mutalik et al., 2020; Schutte-Smith et al., 2023).

The antimicrobial activity of *Staphylococcus aureus* NPS has been extensively studied with human pathogenic bacteria such as *Escherichia coli* (*E. coli*) and *Staphylococcus aureus* (Moradpoor et al., 2021). The bactericidal activity of NPS depends on factors such as size, stability, and concentration in the growth medium. When grown in medium enriched with NPS, the growth of bacterial populations can be inhibited by specific interactions with the nanoparticles (Moustafa et al., 2021). In general, the size of bacterial cells is in the micrometer range, while their cell membranes have pores in the nanometer range. NPS have the unique ability to penetrate the cell membrane because they are smaller than the pores of bacteria.

Currently, nanocrystalline titanium dioxide (TiO_2) is a semiconductor known for its photocatalytic activity (Andreas et al., 2022; Eddy et al., 2023; Oemar et al., 2023). In addition, TiO_2 has great potential as an auto-cleaning and disinfecting agent in various applications. TiO_2 has been widely used to kill

various groups of microorganisms, including bacteria, fungi, and viruses, due to its high photoreactivity, diverse antibiosis, and chemical stability (Younis et al., 2023; Yuzer et al., 2022). TiO_2 NPS break down organic compounds by releasing hydroxyl radicals and superoxide ions continuously, which is efficient in inhibiting the growth of pathogenic bacteria. The strong oxidizing power of TiO_2 NPS can be used against bacteria and other organic compounds. Leveraging the sol-gel method offers a unique opportunity to tailor the properties of TiO_2 nanoparticles, thereby enhancing their antimicrobial activity.

Recent research endeavors have shed light on the significance of synthesis methods in modulating the properties of TiO_2 nanoparticles and optimizing their performance in antimicrobial applications. For instance, a study conducted by (Phromma et al., 2020) successfully synthesized TiO_2 nanoparticles with a narrow size distribution using a wet ball milling sol-gel method. Their findings underscored the crucial role of calcination temperature in influencing particle size, crystallite size, and phase transition of TiO_2 nanoparticles. Notably, higher calcination temperatures were found to enhance the crystallinity of synthesized TiO_2 and promote the transition to the rutile phase, which significantly impacted the photocatalytic activity of the nanoparticles (Mahy et al., 2021; Phromma et al., 2020).

Furthermore, the incorporation of dopants, such as iron (Fe), into TiO_2 nanoparticles via the sol-gel method has demonstrated promising results in enhancing their photocatalytic efficiency under visible light irradiation. (Mancuso et al., 2023) employed a reverse-micelle sol-gel method to prepare Fe-doped TiO_2 samples for the photodegradation of crystal violet dye. Their comprehensive characterization of the photocatalysts revealed the successful introduction of Fe into the titania matrix, leading to the modulation of the relative amounts of TiO_2 polymorphs and a reduction in the band gap energy. This innovative approach not only broadens the spectrum of TiO_2 photocatalytic applications but also underscores the versatility of the sol-gel method in tailoring the properties of TiO_2 nanoparticles for specific antimicrobial purposes (Ali et al., 2021; Nachit et al., 2022). Moreover, the eco-friendly colloidal aqueous sol-gel synthesis of TiO_2 presents a promising avenue for producing crystalline TiO_2 nanoparticles without the need for a calcination step. This method offers distinct advantages, including the ability to obtain crystalline TiO_2 nanoparticles with tailored morphology and crystallinity while minimizing the use of organic chemicals. Studies have highlighted the comparable photocatalytic efficiency of colloidal aqueous TiO_2 nanoparticles to conventionally synthesized counterparts, indicating their potential for various antimicrobial applications and beyond (Mahy et al., 2021).

Previously, a discussion of the sol-gel method to increase the antimicrobial activity of titania nanoparticles was described in depth. However, although much research has been carried out on the physical, chemical and biological properties of TiO_2 (Mutalik et al., 2020; Rachmaniar et al., 2024; Schutte-Smith et al., 2023), research on in-vitro testing of the antimicrobial properties of TiO_2 NPS is still very limited. Therefore, this study was designed to evaluate the antimicrobial activity of TiO_2 NPS synthesized by the sol-gel method. The prepared TiO_2 NPS samples will be tested against various microbes such as Gram-positive bacteria: *Staphylococcus aureus*, Gram-negative bacteria: *Escherichia coli* (*E. coli*), and the test fungal pathogen: *Aspergillus penicillioides*.

2. EXPERIMENTAL SECTION

2.1 Materials

The materials utilized in the preparation of TiO_2 nanoparticle samples via the sol-gel technique included titanium isopropoxide raw material (TTIP 99% precursor) sourced from Sigma Aldrich Singapore, 3.2 mL of 4.4 M HNO_3 (pH 0.6), and ethanol solvent (C_2H_5OH, Merck India).

2.2 Methods

TiO_2 nanoparticle samples were prepared via sol-gel technique with titanium isopropoxid raw material (TTIP 99% precursor, Sigma Aldrich Singapore) and ethanol solvent. The synthesis of TiO_2 NPS begins by mixing 5 mL of TTIP with 5 mL of ethanol. The solution (sol A) was stirred for 30 minutes at 1500 rpm at room temperature. Solution (sol B) was prepared by dissolving 6 mL of ethanol, and adding 3.2 mL of 4.4 M HNO_3 (pH 0.6). The solution was then stirred for 20 minutes at 1500 rpm and room temperature. Next, dripping the solution of sol B into sol A at 1500 rpm. The mixture was then hydrolyzed at 40°C for one hour to produce a yellow solid. The solid was then ball milled at 192 rpm. TiO_2 NPS powder is then dried in the oven to remove impurities that still exist, followed by heating at 400°C for 2 hours. The illustration scheme of TiO_2 NPS synthesis experiments with Sol-gel method is presented in Figure 1.

2.3 Characterization of TiO_2 NPS

The sintered TiO_2 NPS powder was then characterized for morphology and particle size by field-emission scanning electron microscopy (FESEM; Quanta FEG 650, FEI USA). X-ray diffraction (XRD) analysis (X'Pert3 Powder, PANalytical Company B.V. Netherlands) was performed at 2θ angles in the range of 11°-90° to determine the crystalline phases formed. The phase analysis of the TiO_2 nanoparticles was based on COD 2310710 for anatase phase, COD 9004142 for rutile phase, and AMCSD 0005160 for brokite phase. The proportions of the anatase and rutile phases were calculated by the Rietveld Method using Rietica software.

2.4 Microorganism Source

As for the preparation of TiO_2 NPS suspension, microbial strains were obtained from the microbial type culture collection (BM-UM), Department of Biology, State University of Malang. Stock cultures of various Gram-negative bacteria: *E. coli* (BM-UM No: 87), Gram-positive: *Staphylococcus aureus* (BM-UM No: 91) and the fungus *Aspergillus penicillioides*

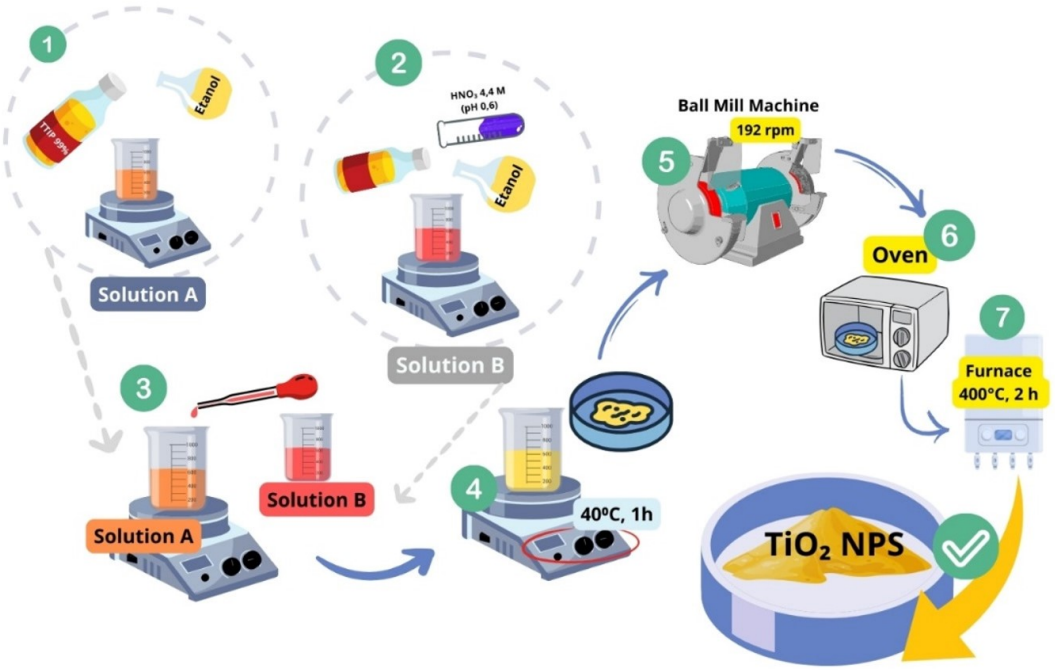

Figure 1. Illustration of TiO_2 Experimental Method using Sol-Gel Method

(BM-UM No: 117) were subcultured and maintained in sugar solution. Preparation of TiO_2 NPS solutions of 0.1, 0.15, 0.2, and 0.25 g/mL. The TiO_2 NPS solution was stirred at 300 rpm for 30 minutes at room temperature.

2.5 Antimicrobial Activity Test

Antimicrobial activity of TiO_2 NPS synthesized against Gram-positive bacteria *Staphylococcus aureus*, Gram-negative bacteria *E. coli*, and fungus *Aspergillus penicillioides*. Kirby-Bauer disc diffusion method was used for antimicrobial test (Moradpoor et al., 2021). Using sterile cotton swabs, cultures of test organisms were made on petri dishes for hygiene. It was then left for 30 minutes to absorb the culture. Then, wells with a diameter of 6 mm were pressed onto the petri dish to test the antimicrobial activity of the TiO_2 NPS sample. The wells were sealed with one drop of melted agar (0.8% agar) to prevent leakage of nanomaterials from the bottom of the wells. Using a pipette, 1 mL of each sample at various concentrations (0.1, 0.15, 0.2, and 0.25 g/mL) of TiO_2 NPS solution was poured into each well on a Petri dish. After that, the Petri dish that has been given TiO_2 is incubated at room temperature for a period of 12-24 hours in both dark and visible light conditions and then measured the diameter. The illustration scheme of TiO_2 NPS anti-microbial testing is presented in Figure 2.

3. RESULTS AND DISCUSSIONS

Morphology and size distribution of TiO_2 NPS characterized using SEM instrument. The results of characterization are presented in Figure 1. The Figure 1 shows TiO_2 NPS experiencing agglomeration. Based on previous research, it was revealed that agglomeration in TiO_2 is caused by electrostatic forces between particles (Listanti et al., 2019) because basically TiO_2 NPS has properties easily aggregated (Taufiq et al., 2019).

SEM images of the TiO_2 NPS are shown in Figure 3, which were taken at different magnifications of 20K×, and 60K× (Figure 3b and Figure 3c). From the SEM images (Figure 3b and 3c), it is known that the shape looks like a ball that stacks like a cereal granule. This result is proven from several previous studies that TiO_2 is spherical shaped like a ball. The size of some granules varies. The particle size distribution from 20k magnification was found to be 124.32 nm. These results indicated the presence of a phase coincide between anatase, rutile and brokite. The difference in phase formed is evidenced by the size of the particles formed. Anatase has a tendency to form small balls that stack on top of each other, while rutile and brokite have a larger diameter size. Figure 3 as a whole shows uniformity. Even if the many particles created cause agglomeration, it still has a homogeneous size level between particles. TiO_2 NPS are essentially polycrystalline, and this will be discussed further in the XRD results.

The optimum particle size reflects high stability against gravity due to Brownian motion and affects the release, bioavailability and organoleptic properties of nanoparticles (Liao et al., 2020; Rahmawati et al., 2020). The negative zeta potential of TiO_2 NPS synthesized using the USP method showed more uniform particles than other methods. This is stated by previous research that TiO_2 NPS have a high degree of heterog-

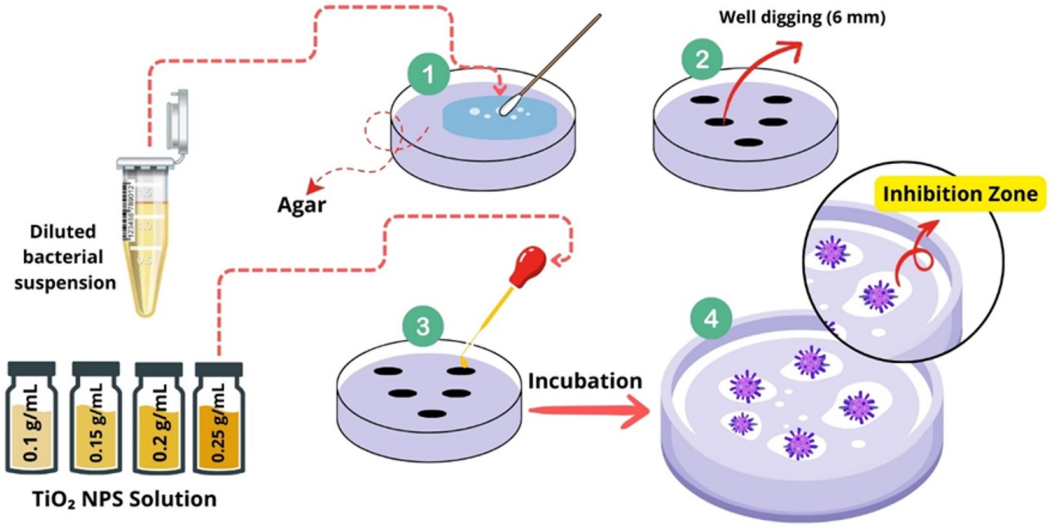

Figure 2. Schematic Illustration of Anti-Microbial Activity Testing

enization so that it requires other methods that can gradually compose TiO_2 NPS particles. The results of this study then prove that the USP method can improve the homogeneity of TiO_2 NPS because TiO_2 is arranged gradually from the formation flow. Figure 3a and Figure 3b show a higher negativity in the charge, giving greater stability to the synthesized TiO_2 NPS, thus avoiding excessive buildup of particles (Anwar et al., 2023).

Furthermore, XRD characterization was carried out to strengthen the presence of a polycrystalline phase in TiO_2 NPS. These results can be seen in Figure 4. Basically, the diffraction pattern of TiO_2 NPS has crystalline peak characteristics that vary depending on the phase. This can be seen from the research results in Table 1. The majority of peaks are known to belong to the rutile phase. This peak is confirmed by the research of Rachmaniar et al. (2024) which identified that the brokite peak is located TiO_2 NPS at an angle of 2θ = 27.48°. The same thing was also reported by David et al. which states that the main peak of TiO_2 NPS rutile is located at an angle of 2θ = 27.47° with TiO_2 samples (Aboubakr et al., 2021). In addition to rutile high peak is also owned by brokite which is at 2θ = 56.19°. However, from Figure 4 the peaks belonging to rutile and brokite are slightly the same, making it difficult to determine the main peak of brokite. This is because the annealing temperature used in the synthesis is in the phase transition of rutile and brokite, which is 400°C. Ismail et al. (2023) stated that TiO_2 will begin to have brokite particles when annealing has been at 400°C, while the dominant peak of the brokite phase is at 500°C. Detailed percentage of phases formed can be seen in Table 1.

The results of the XRD diffraction pattern of TiO_2 NPS are then smoothed using the Rietveld method to determine the crystal structure and particle size that matches the data COD 2310710 for anatase, COD 9004142 for rutile, and amcsd 0005160 for brokite so that the smoothing results are shown in Figure 4a. Based on the analysis manual using Rietica software, the parameter values are Rp, Rwp, Rb, and GoF (X^2) which are used to estimate the fit between the data and the model during the refinement process showed in Table 2.

Table 1. Diffractogram peaks of TiO_2 NPS

2 Theta (deg.)	Peak position of hkl
25.38	[011]
27.48	[110]
35.9	[102]
39.18	[020]
41.29	[111]
44.1	[120]
54.36	[121]
56.19	[113]
62.78	[024]
64.11	[023]
69.11	[116]
69.95	[112]
82.56	[231]

As previously known, TiO_2 has anatase, rutile and brokite structures. In general, there are 6 parts filled with tetrahedral Ti^{4+} ions in anatase, 9 parts filled with tetrahedral Ti^{4+} ions in rutile, and 8 parts of octahedral Ti^{4+} ions in brokite (Ali et al., 2020). Crystal structure model of TiO_2 NPS visualized

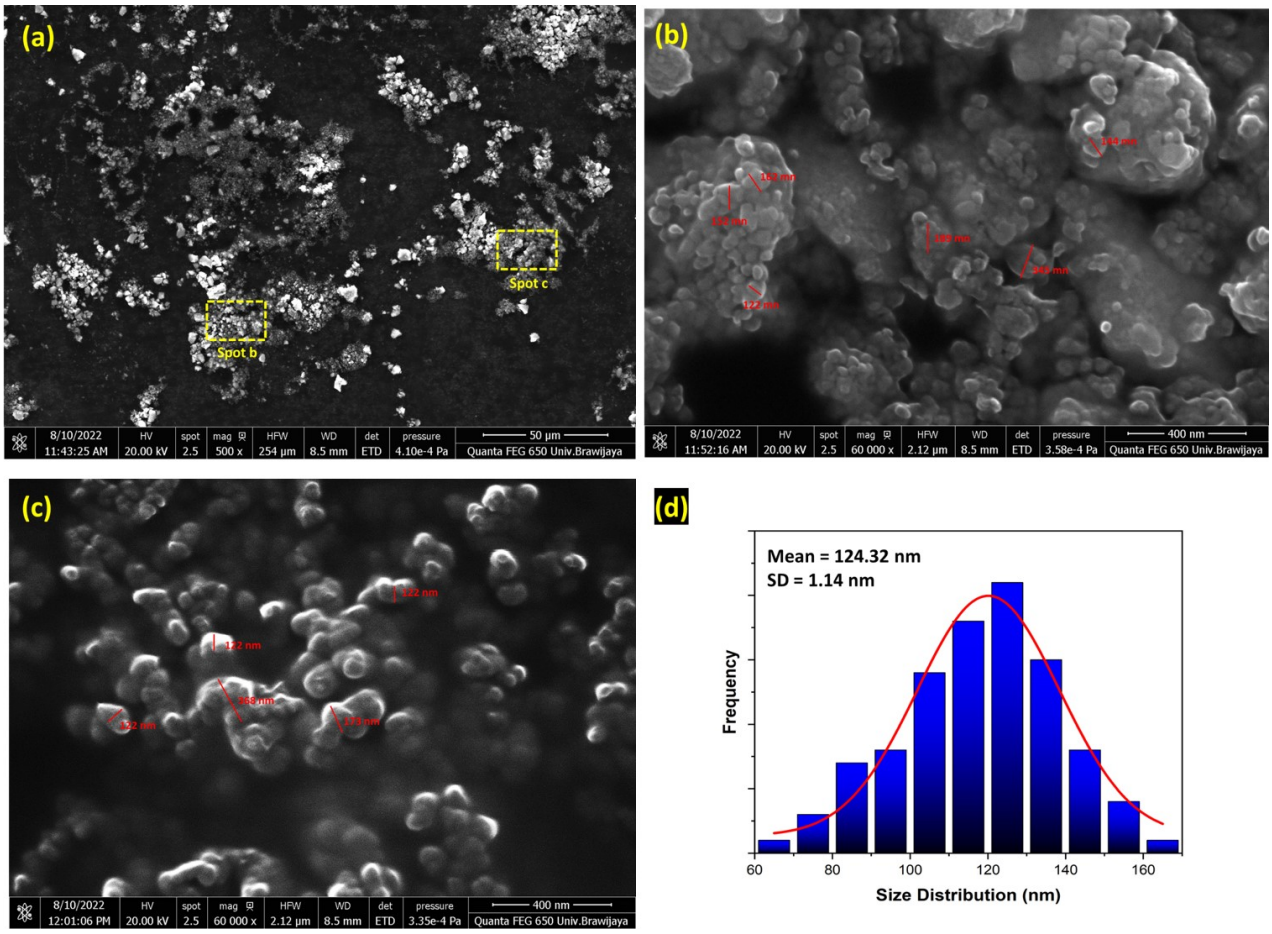

Figure 3. SEM Characterization Results of TiO_2 NPS with (a) 20K× Magnification, (b and c) 60K× Magnification, and (d) Particle Size Distribution from 60K× Magnification

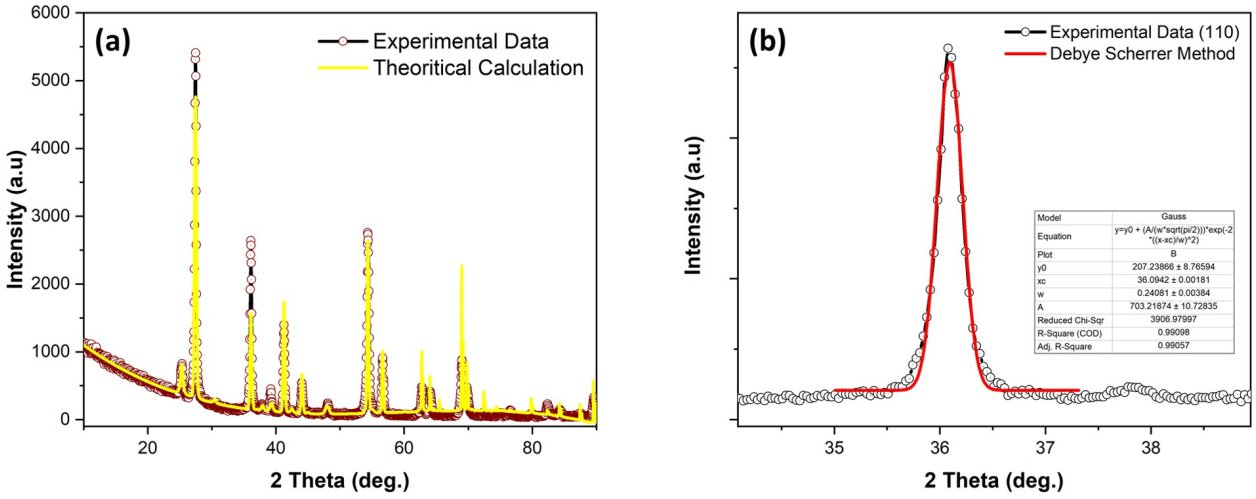

Figure 4. XRD Diffraction Pattern Results TiO_2 NPS that has been in (a) Refinement and (b) in Fitting using the Debye-Scherrer Equation

Table 2. TiO_2 NPS Refinement Results Output

Parameter	Value	Parameter	Value
Crystallite Size (nm)		Lattice Constant Anatase (Å)	
Anatase	118.71	a^2	3.78
Rutile	244.13	c	9.48
Brokite	28.19	Lattice Constant Rutile (Å)	
Unit Volume (Å3)		a^2	4.59
Anatase	136.05	c	2.96
Rutile	62.46	Lattice Constant Brokite (Å)	
Brokite	266.72	a	9.54
% Fase		b	5.34
Anatase	5.35	c	5.21
Rutile	51.61		
Brokite	43.05		
Rp	18.13		
Rwp	9.98		
X^2	6.71		
Brag-Factor	10.53		

through Vesta software. Based on the software, the TiO_2 NPS crystal structure obtained is appropriate and can be seen in Figure 5.

In addition to the refinement method, there is a similar method used to confirm the crystal grain size with a different approach, namely using the Debye-Scherrer fitting method shown in Figure 5b. This method uses the Debye-Scherrer equation listed in Equation 1. The Debye-Scherrer fitting method is used to estimate the crystal grain size based on XRD diffraction patterns (Žerjav et al., 2022). In this method, the diffraction patterns are fitted to the Debye-Scherrer equation to generate parameters such as crystal grain size and stress strain in the grains.

By performing a good fitting between the observed diffraction pattern and the Debye-Scherrer equation, a more accurate estimate of the grain size of the crystal is obtained. By using the Debye-Scherrer fitting method, more accurate identification and confirmation of the crystal grain size present in the sample is obtained (Mustapha et al., 2021). Thus, the Debye-Scherrer fitting method is one of the useful and commonly used methods to confirm the crystal grain size in XRD diffraction pattern analysis (Mustapha et al., 2021):

$$D = \frac{K\lambda}{\beta \cos\theta} \quad (1)$$

Where D as the size of the crystal grain, λ as the wavelength of X-rays, β is the FWHM at the maximum peak, θ is the Bragg angle and K is a constant with a value of 0.9. With the Debye-Scherrer equation, the TiO_2 NPS sample has a particle size of 128 nm. These results confirm that the majority of TiO_2 NPS formed in the form of rutile with the highest level of crystal size compared to other phases. These results are also well confirmed by Yang et al. which states that TiO_2 with annealing temperature of 400°C has a dominant rutile phase.

Furthermore, anti-bacterial testing was carried out on TiO_2 samples with variations in TiO_2 mass. Tests were carried out using a variety of bacteria *S. aureus* and *E. coli*. While the fungal pathogen using *Aspergillus penicillioides* with variations in concentration. The test results are presented in Figure 6.

Based on Figure 6a, it is known that TiO_2 has the highest inhibition zone of 2.03 mm for *S. aureus* bacteria and 0.117 mm for *Escherchia coli* bacteria and fungal pathogen *Aspergillus penicillioides* which is 19.9 mm for concentration variation of 0.1 g/mL. The presence of TiO_2 acts as a link between Ti^{4+} and microorganisms. TiO_2 nano particles proved to have less significant impact in killing bacteria. This is explained in the empirical fact that TiO_2 has the ability to damage cell walls but the effect is higher when composite using Ag which is proven to be more effective in killing bacteria (Nikmah et al., 2021). However, TiO_2 is more effective in damaging fungal tissue. Evident from the results of antimicrobial characterization, the inhibition zone value of fungi is higher than bacteria.

TiO_2 has a unique ion, namely Ti^{4+}. This causes TiO_2 to have electrons in its crystal structure, which then forms electron-hole pairs (Nachit et al., 2022). These free electrons and holes are then involved in redox reactions with surrounding water and oxygen molecules, producing hydroxyl radicals (OH) and superoxide radicals (O^{2-}). These radicals are highly reactive and can damage bacterial cell membranes, resulting in oxidation of membrane lipids and DNA damage (Alghamdi et al., 2022). This process causes an antimicrobial effect that reduces or eliminates the bacterial population around TiO_2. In addition, the effect of TiO_2 nanoparticles also increases the effectiveness of damage to bacteria. This is evidenced from previous research that micro-sized TiO_2 has no inhibition or

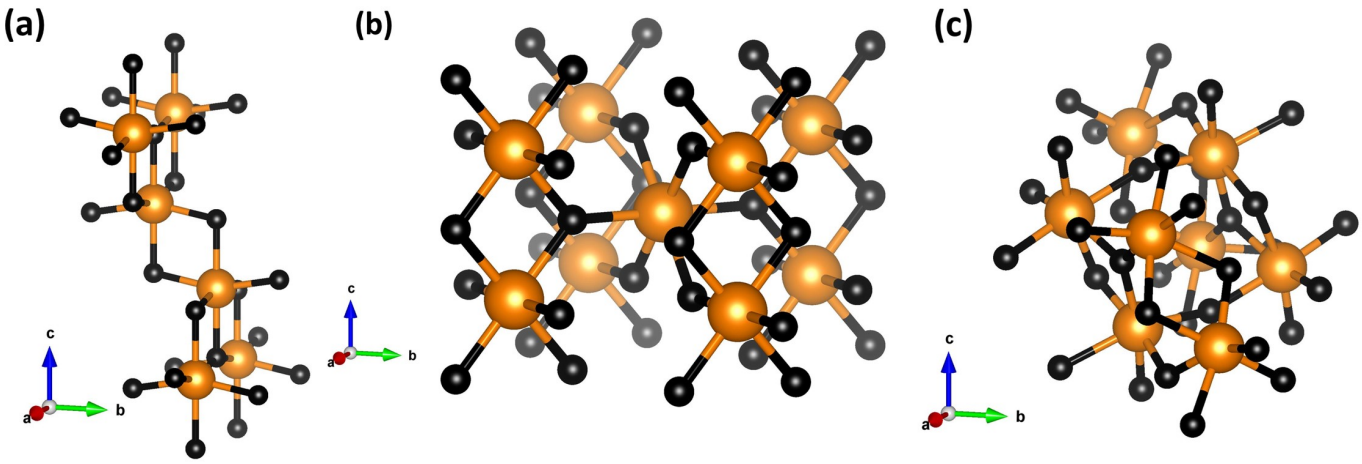

Figure 5. Crystal Structure of TiO_2 NPS (a) Anatase, (b) Rutile, (c) Brokite

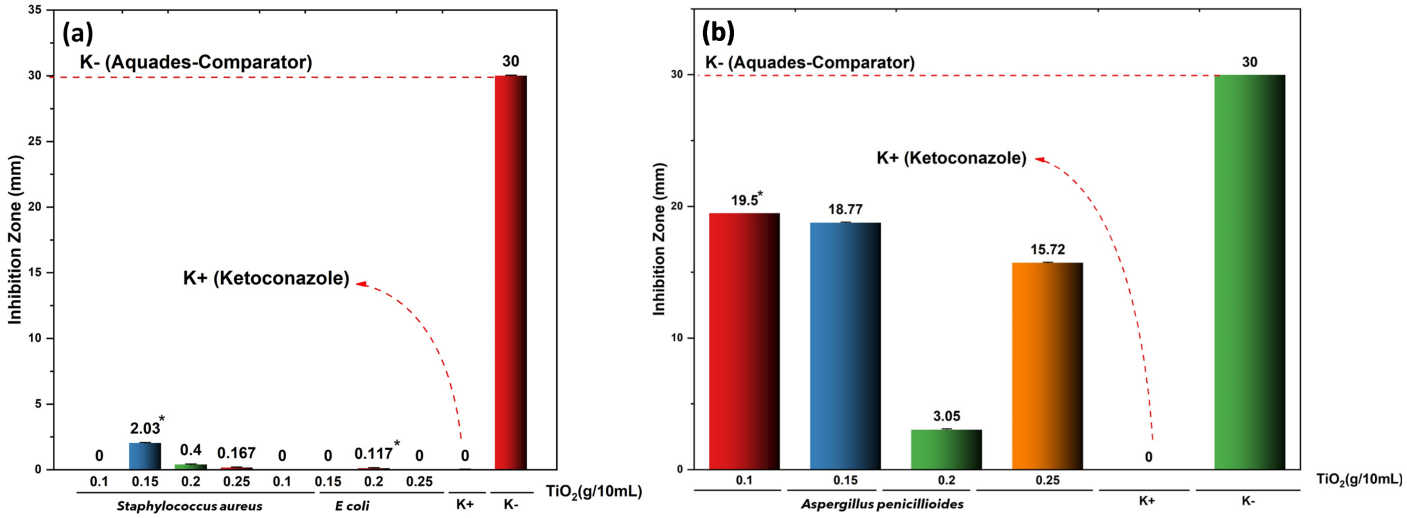

Figure 6. Characterization Results of TiO_2 NPS (a) Anti-Microbial and (b) Anti-Fungal

is less effective in killing *E. coli* bacteria.

Furthermore, TiO_2 has an influence on cell damage by disrupting cellular donor ligands. This process results in the release of Ti^{4+} into the cytoplasm and increases the formation of ROS (Reactive Oxygen Species) (Mustapha et al., 2021; Nikmah et al., 2021; Yuzer et al., 2022). ROS will play a key role in oxidative activity resulting in cells failing to maintain normal physiology and damage to cell function (Aboubakr et al., 2021). The placement of TiO_2 nanoparticles has contributed to the formation of free radical formation due to oxidative stress (Ali et al., 2020). TiO_2 will tend to associate with soft acids such as sulfhydryl groups (R-SH) present in proteins. As a result, the toxicity of TiO_2 will increase and damage cells by denaturing proteins (Fan et al., 2020). The mechanism of cell damage caused by TiO_2 is described by Figure 7.

4. CONCLUSIONS

TiO_2 NPS results show morphology that tends to agglomerate. This is consistent with previous findings which state that agglomeration on TiO_2 is caused by electrostatic forces between particles. The results of SEM characterization of TiO_2 NPS look spherical shape that stacked each other, indicating the presence of a phase coincide between anatase, rutile, and brokite. Furthermore, the results of X-ray diffraction analysis confirmed the presence of these phases, with the majority of diffraction peaks associated with the rutile phase. The Debye-Scherrer fitting method also estimated the crystal grain size to be around 128 nm, indicating the dominance of the rutile phase in the sample. Antimicrobial testing showed that TiO_2 has a more effective antimicrobial effect against fungi than bacteria, with the mechanism of cell damage involving the formation

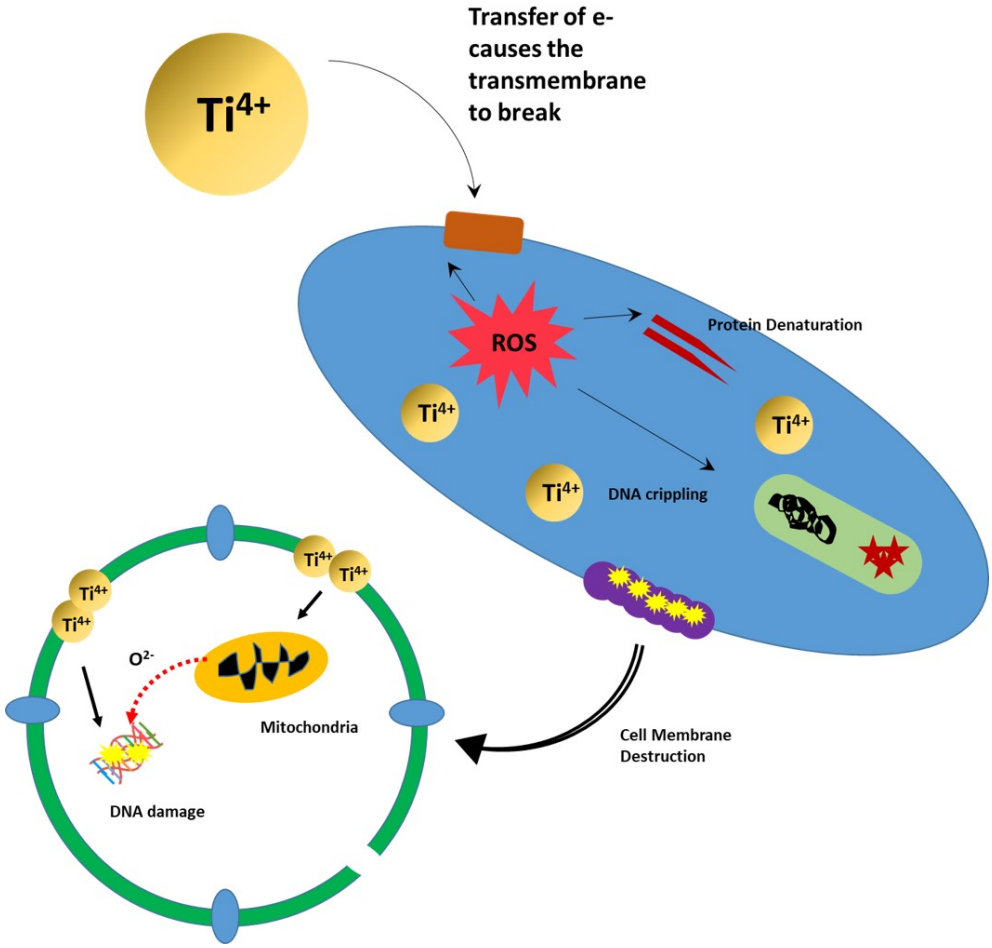

Figure 7. Mechanism of Microbial Cell damage

of free radicals such as hydroxyl and superoxide radicals. Although TiO_2 is less effective in killing bacteria directly, TiO_2 nanoparticles increase the effectiveness of damage to bacteria through oxidation processes that damage bacterial cell membranes and DNA. This shows the potential application of TiO_2 as an effective antimicrobial agent, especially against fungi.

5. ACKNOWLEDGMENT

We thank to LPPM Universitas Negeri Malang for Research Grant Based on Decree Number State University of Malang and Agreement/Contract Number 10.5.60/UN32.20.1/LT/2023 to receive the Budget Riset Kolaborasi Indonesia (RKI) Scheme A for 2023.

REFERENCES

Aboubakr, M., S. M. Elshafae, E. Y. Abdelhiee, S. E. Fadl, A. Soliman, A. Abdelkader, M. M. Abdel-Daim, K. A. Bayoumi, R. S. Baty, and E. Elgendy (2021). Antioxidant and Anti-inflammatory Potential of *Thymoquinone* and *Lycopene* Mitigate the Chlorpyrifos-induced Toxic Neuropathy. *Pharmaceuticals*, **14**(9); 940

Ahmadpour Kermani, S., S. Salari, and P. Ghasemi Nejad Almani (2021). Comparison of Antifungal and Cytotoxicity Activities of Titanium Dioxide and Zinc Oxide Nanoparticles with Amphotericin B against Different Candida Species: In Vitro Evaluation. *Journal of Clinical Laboratory Analysis*, **35**(1); e23577

Albukhaty, S., L. Al-Bayati, H. Al-Karagoly, and S. Al-Musawi (2022). Preparation and Characterization of Titanium Dioxide Nanoparticles and In Vitro Investigation of Their Cytotoxicity and Antibacterial Activity against *Staphylococcus aureus* and *Escherichia coli*. *Animal Biotechnology*, **33**(5); 864–870

Alghamdi, H. M., M. M. Abutalib, A. Rajeh, M. A. Mannaa, O. Nur, and E. M. Abdelrazek (2022). Effect of the Fe_2O_3/TiO_2 Nanoparticles on the Structural, Mechanical, Electrical Properties and Antibacterial Activity of the Biodegradable Chitosan/Polyvinyl Alcohol Blend for Food Packaging. *Journal of Polymers and the Environment*, **30**(9); 3865–3874

Alhagri, I. A., T. F. Qahtan, M. O. Farea, A. N. Al-Hakimi, S. M. Al-Hazmy, S. E.-S. Saeed, and A. E. Albadri (2023).

Enhanced Structural, Optical Properties and Antibacterial Activity of PEO/CMC Doped TiO_2 NPs for Food Packaging Applications. *Polymers*, **15**(2); 384

Ali, G. W., O. W. Guirguis, M. Gobara, S. F. M. Mustafa, N. A. El-Zaher, and W. I. Abdel-Fattah (2020). On the Optical Characterization and Biological Implications of Titania Phases. *Optical Materials*, **109**; 110269

Ali, M. M., M. J. Haque, M. H. Kabir, M. A. Kaiyum, and M. S. Rahman (2021). Nano Synthesis of ZnO–TiO_2 Composites by Sol-gel Method and Evaluation of Their Antibacterial, Optical and Photocatalytic Activities. *Results in Materials*, **11**; 100199

Andreas, Irmanto, and A. Oktaviani (2022). Synthesis, Characterization, and Activity of The Photocatalyst Polyaniline (PANI)/TiO_2 in Degrading Rhodamine B Dye. *Science and Technology Indonesia*, **7**(1); 126–131

Anwar, N., M. A. Iqbal, M. Ahmed, B. Anwar, I. Abbas, S. T. Iqbal, F. Anwar, N. Mushahid, R. Y. Capangpangan, and A. C. Alguno (2023). Analyzing pH-dependent Structural Characteristics and Optical Transmittance of Titanium Dioxide. *Zeitschrift Für Naturforschung A*, **78**(3); 297–303

Eddy, D. R., M. D. Permana, L. K. Sakti, G. A. N. Sheha, H. Solihudin, T. Takei, N. Kumada, and I. Rahayu (2023). Heterophase Polymorph of TiO_2 (Anatase, Rutile, Brookite, TiO_2 (B)) for Efficient Photocatalyst: Fabrication and Activity. *Nanomaterials*, **13**(4); 1–31

Fan, L., F. Wang, D. Zhao, X. Sun, H. Chen, H. Wang, and X. Zhang (2020). Two Cadmium(II) Coordination Polymers as Multi-Functional Luminescent Sensors for the Detection of Cr(VI) Anions, Dichloronitroaniline Pesticide, and Nitrofuran Antibiotic in Aqueous Media. *Spectrochimica Acta Part A: Molecular and Biomolecular Spectroscopy*, **239**; 118467

Halizah, S. N., Sunaryono, and N. M. Chusna (2023). Magnetic Properties and Antibacterial Activity of Fe_3O_4@ZnO/TiO_2 Core-shell Nanocomposites against *Staphylococcus aureus*. *AIP Conference Proceedings*, **2687**(1); 050030

Ismail, B. A., Z. H. Abd El-Wahab, O. A. M. Ali, and D. A. Nassar (2023). Synthesis, Structural Characterization, and Antimicrobial Evaluation of New Mononuclear Mixed Ligand Complexes Based on Furfural-Type Imine Ligand, and 2,2'-Bipyridine. *Scientific Reports*, **13**(1); 9196

Liao, C., Y. Li, and S. C. Tjong (2020). Visible-Light Active Titanium Dioxide Nanomaterials with Bactericidal Properties. *Nanomaterials*, **10**(1); 124

Listanti, A., A. Taufiq, A. Hidayat, N. Hidayat, H. Susanto, and S. Soontaranon (2019). Synthesis, Structural and Toxicity Characters of Nano-sized Titanium Dioxide/Magnetite Nanoparticles. *IOP Conference Series: Materials Science and Engineering*, **515**(1); 012057

Mahy, J. G., L. Lejeune, T. Haynes, S. D. Lambert, R. H. M. Marcilli, C.-A. Fustin, and S. Hermans (2021). Eco-Friendly Colloidal Aqueous Sol-Gel Process for TiO_2 Synthesis: The Peptization Method to Obtain Crystalline and Photoactive Materials at Low Temperature. *Catalysts*, **11**(7); 768

Mancuso, A., N. Blangetti, O. Sacco, F. S. Freyria, B. Bonelli, S. Esposito, D. Sannino, and V. Vaiano (2023). Photocatalytic Degradation of Crystal Violet Dye under Visible Light by Fe-Doped TiO_2 Prepared by Reverse-Micelle Sol–Gel Method. *Nanomaterials*, **13**(2); 271

Moradpoor, H., M. Safaei, A. Golshah, H. R. Mozaffari, R. Sharifi, M. M. Imani, and M. S. Mobarakeh (2021). Green Synthesis and Antifungal Effect of Titanium Dioxide Nanoparticles on Oral *Candida albicans* Pathogen. *Inorganic Chemistry Communications*, **130**; 108748

Moustafa, H., A. E.-M. Karmalawi, and A. M. Youssef (2021). Development of Dapsone-capped TiO_2 Hybrid Nanocomposites and Their Effects on the UV Radiation, Mechanical, Thermal Properties and Antibacterial Activity of PVA Bionanocomposites. *Environmental Nanotechnology, Monitoring & Management*, **16**; 100482

Mustapha, S., J. O. Tijani, M. M. Ndamitso, A. S. Abdulkareem, D. T. Shuaib, A. T. Amigun, and H. L. Abubakar (2021). Facile Synthesis and Characterization of TiO_2 Nanoparticles: X-ray Peak Profile Analysis Using Williamson–Hall and Debye–Scherrer Methods. *International Nano Letters*, **11**(3); 241–261

Mutalik, C., Y. Hsiao, Y. Chang, D. I. Krisnawati, M. Alimansur, A. Jazidie, M. Nuh, C. Chang, D. Wang, and T. Kuo (2020). High UV-Vis-NIR Light-Induced Antibacterial Activity by Heterostructured TiO_2−FeS_2 Nanocomposites. *International Journal of Nanomedicine*, **15**; 8911–8920

Nachit, W., H. Ait Ahsaine, Z. Ramzi, S. Touhtouh, I. Goncharova, and K. Benkhouja (2022). Photocatalytic Activity of Anatase-brookite TiO_2 Nanoparticles Synthesized by Sol Gel Method at Low Temperature. *Optical Materials*, **129**; 112256

Nikmah, A., A. Taufiq, A. Hidayat, Sunaryono, and H. Susanto (2021). Excellent Antimicrobial Activity of Fe_3O_4/SiO_2/Ag Nanocomposites. *Nano*, **16**(05); 2150049

Oemar, B., A. Arifin, D. Bahrin, D. Ramadhan, M. A. Rifqy, M. R. Tinambunan, et al. (2023). Experimental Investigation on Thermophysical and Stability Properties of TiO_2/Virgin Coconut Oil Nanofluid. *Science and Technology Indonesia*, **8**(2); 178–183

Phromma, S., T. Wutikhun, P. Kasamechonchung, T. Eksangsri, and C. Sapcharoenkun (2020). Effect of Calcination Temperature on Photocatalytic Activity of Synthesized TiO_2 Nanoparticles via Wet Ball Milling Sol-Gel Method. *Applied Sciences*, **10**(3); Article 3

Rachmaniar, S., D. A. Nugraha, D. J. D. H. Santjojo, R. T. Tjahjanto, N. Mufti, and Masruroh (2024). Prevention of Particle Agglomeration in Sol–Gel Synthesis of TiO_2 Nanoparticles via Addition of Surfactant. *Journal of Nanoparticle Research*, **26**(3); 45

Rahmawati, S., A. Taufiq, A. Hidayat, A. Nikmah, Sunaryono, and Masruroh (2020). Green Synthesis of Fe_3O_4 Nanoparticles Based on Biosurfactant *Saccharum Officinarum* Extract. *AIP Conference Proceedings*, **2251**(1); 040035

Schutte-Smith, M., E. Erasmus, R. Mogale, N. Marogoa, A. Jayiya, and H. G. Visser (2023). Using Visible Light to Activate Antiviral and Antimicrobial Properties of TiO_2 Nanoparticles in Paints and Coatings: Focus on New Developments for Frequent-Touch Surfaces in Hospitals. *Journal of Coatings Technology and Research*, **20**(3); 789–817

Sumardi, Masfria, M. Basyuni, and A. W. Septama (2022). Potential of Polyisoprenoid of Mangroves as Antimicrobial and Anticancer: A Bibliometric Analysis. *Science and Technology Indonesia*, **7**(1); 22–28

Taufiq, A., D. Arista, Sunaryono, R. E. Saputro, N. Hidayat, S. Soontaranon, E. Handoko, and D. Darminto (2019). Investigation of Structural and Antifungal Behaviors of Nano-Sized Anatase TitaniumDioxide Synthesized by Co-Precipitation Route. *Materials Science Forum*, **966**; 181–188

Younis, A. B., Y. Haddad, L. Kosaristanova, and K. Smerkova (2023). TitaniumDioxide Nanoparticles: Recent Progress in Antimicrobial Applications. *WIREs Nanomedicine and Nanobiotechnology*, **15**(3); e1860

Yuzer, B., M. I. Aydın, A. H. Con, H. Inan, S. Can, H. Selcuk, and Y. Kadmi (2022). Photocatalytic, Self-cleaning and Antibacterial Properties of Cu(II) Doped TiO_2. *Journal of Environmental Management*, **302**; 114023

Žerjav, G., K. Žižek, J. Zavašnik, and A. Pintar (2022). Brookite vs. Rutile vs. Anatase: What's Behind Their Various Photocatalytic Activities? *Journal of Environmental Chemical Engineering*, **10**(3); 107722

